Numerical verification of the condenser finite volume model

Numerical verification of the condenser finite volume model

Michael Giovannini, Marco Lorenzini

Università di Bologna, DIN – Dipartimento di Ingegneria Industriale, Via Fontanelle 40, I-47121, Forlì (FC) Italy

E-mail: marco.lorenzini@unibo.it

Abstract. Numerical modelling of vapour compression systems is very useful for performance optimization through the implementation of suitable model-based control applications; in this context the heat exchangers are the most challenging component to devise, due to phase transition and ensuing discontinuities of the physical properties, and one tool which has proven itself suitable for the task is the finite volume method. A numerical verification of a finite volume model of a brazed plate condenser in counterflow arrangement is carried out, employing a fixed timestep solver; some useful guidelines are suggested to properly choose the solver order, the integration step size and the number of grid elements, balancing the accuracy of the predictions with computational time and model stability and flexibility during the transients, with the ultimate goal to provide a model suited for real-time simulations and control-oriented applications.

1. Introduction

It is estimated that about 5 billion refrigeration systems are in operation worldwide, responsible for about 20% of the global energy demand, and this figure is expected to more than double by 2050, mostly owing a steady growth of air conditioning systems [1]. Vapour compression systems (VCSs) are the most widespread technology in Heating, Ventilating, Air-Conditioning and Refrigeration (HVAC&R). In these systems a working fluid (refrigerant) is recirculated between two sections in which it exchanges thermal energy with two environments at different temperatures; the sections are kept at different pressure through the action of a compressor and an expansion valve. Numerical modelling of VCSs can be a promising way to improve their energy efficiency, through better system design and the implementation of suitable control strategies; in this way is possible to contain both energy consumption and greenhouse gas (GHG) emissions.

To model VCSs under unsteady conditions, the largest effort must be devoted to the heat exchangers for two reasons:

- the dynamic behaviour of the VCSs is strongly affected by the thermal transients, because the time scale of the heat transfer is dominant by order of magnitude respect to the mechanical one [2];
- the heat transfer rates and the pressure levels are coupled because the working fluid undergoes a non-instantaneous phase transition

According to [3], heat exchanger models can be classified into three categories: lumped parameter, moving boundary and finite volume. These techniques mainly differ in their approach to domain discretization: indeed, the process can be described employing a single control volume, for which the balance equations for mass, energy and momentum are written; the estimation of the heat transfer rate is therefore based on the physical properties averaged over the control volume, which coincides with the whole heat exchanger in the lumped-parameter approach. At the other end, in the finite volume (FV) approach the same balance equations are applied to an arbitrary number of cells of the same size; in this way, the properties of the fluids can be evaluated more precisely, reaching an almost local estimate when the grid becomes fine enough. In the middle, the the moving boundary (MB) approach, developed in the last decades, has the aim of combining the accuracy and flexibility of the FV scheme and the low computational cost of a lumped parameter approach. Indeed, since the early realizations of the MB scheme [4], the heat exchanger volume is divided into a maximum of three lumped systems, depending on the phase of the working fluid (superheated vapour, two-phase mixture or subcooled liquid). In this approach the length of each zone can vary in time, depending on the operating conditions, leading to numerical failure as a result of attempting to invert a singular matrix when a zone length goes to zero. To overcome this difficulty, some *representations*, [5], or *modes*, [6], are introduced, and, as a consequence, some switching methodology are needed to move between them during the transients.

On the other hand, the FV formulation has been proved to be more flexible and robust: indeed, it has been succesfully employed to simulate for large transients of an air-cooling evaporator during compressor startup and shutdown, in order to evaluate the effect of the expansion valve opening or closing in this scenario [7]. Recently, the FV formulation was adopted for the simulation of a reversible heat pump during working mode switch, and was successful in dealing with the inversion of the working fluids' arrangement [8].

The FV model of a shell-and-tube heat exchanger employed in the simulation of a whole VCS is numerically verified and experimentally validated in [9]; among other aspects, the work focused on the mesh refinement, integration order and step size effect on the accuracy of the model, highlighting a small mass imbalance during the transients.

Recently, an in depth comparison between the FV formulation and the SMB approach was carried out, [10]; despite the notion that a greater level of discretization leads always to significantly more accurate results, the work demonstrates that in both approaches the numerical error of the predicted values falls into the tolerance of the measured experimental data, with little appreciable differences when the grid is refined.

In this work, the FV model of a brazed-plate (BP) condenser in counterflow arrangement is numerically verified, focusing on the effects of the solver selection on the accuracy of the predicted value of the process variables. The analysis is carried out employing only fixed-step solvers, in order to evaluate the performance of a FV formulation of a heat exchanger, which can be integrated into complex models for real-time simulation and control system design. In this context, also the mesh refinement and the integration step-size are explored to evaluate their effects on the accuracy and stability of the model and on the computational time required.

2. Model definition

In the FV formulation, the heat exchanger is divided into an arbitrary number of cells of the same size. Each control volume includes three elements, the working fluid, the secondary fluid and a portion of the wall of the heat exchanger, for each of which the balance equations may be written.

Some simplifying assumptions are made:

- one-dimensional, compressible and unsteady flow for the working fluid;

- one-dimensional, incompressible steady flow for the secondary fluid;
- cross-sectional area constant for both fluids;
- negligible pressure drops for both fluids;
- negligible axial conduction;
- negligible wall thermal resistance;
- thermal storage in the secondary fluid is neglected.

As a consequence of the assumptions above, the momentum equation is unnecessary for both fluids; moreover, since flow and heat transfer to the secondary fluid are stationary, no differential equation is needed to describe its behaviour, the algebraic equation for heat transfer in each control volume suffices.

In the following, the integral form of the balance equations applied to each control volume (k) for the derivation of the FV formulation are presented.

The refrigerant mass balance equation:

$$V_k \frac{d\rho_k}{d\tau} = \dot{m}_{in,k} - \dot{m}_{out,k} \tag{1}$$

where ρ_k is the average density of the working fluid inside the control volume, V_k is volume occupied by the fluid, and $\dot{m}_{k,in}$ e $\dot{m}_{k,out}$ are the inlet and outlet mass flow rates respectively.

The internal energy balance for the working fluid:

$$V_k \frac{d(\rho_k u_k)}{d\tau} = \dot{m}_{in,k} h_{in,k} - \dot{m}_{out,k} h_{out,k} + \dot{Q}_{r,k} \tag{2}$$

where u_k is the average specific internal energy of the fluid inside the cell, $h_{in,k}$ and $h_{out,k}$ are the specific enthalpies of the fluid at the inlet and outlet and $\dot{Q}_{r,k}$ is the heat transfer rate between the heat exchanger wall in the control volume and the refrigerant.

Finally the wall energy balance:

$$C_{w,k} \frac{dT_{w,k}}{d\tau} = \dot{Q}_{s,k} - \dot{Q}_{r,k} \tag{3}$$

where C_w is the thermal capacity of the wall, $T_{w,k}$ is the wall temperature and $\dot{Q}_{s.k}$ is the heat transfer rate between the secondary fluid and the wall.

A crucial point is the selection of the state variable for the fluid: indeed, two specific and one integral variable are needed for the right characterization of a thermodynamic state. Since volumes are fixed, two intensive state variables must be chosen. Due to the isobaric process assumption, pressure and specific enthalpy may be a convenient choice. Thus, eqs. eqs. (1) to (3), are manipulated according to previous works [7, 11, 12], expanding the time derivative of the density (ρ_k) and the derivative of the internal energy (u_k) as a function of the pressure and the enthalpy applying the chain rule.

$$\frac{d\rho_k}{d\tau} = \frac{\partial \rho_k}{\partial P}\bigg|_{h_k} \frac{dP}{d\tau} + \frac{\partial \rho_k}{\partial h_k}\bigg|_{P} \frac{dh_k}{d\tau} \quad ; \quad \frac{du_k}{d\tau} = \frac{\partial u_k}{\partial P}\bigg|_{h_k} \frac{dP}{d\tau} + \frac{\partial u_k}{\partial h_k}\bigg|_{P} \frac{dh_k}{d\tau} \tag{4}$$

The physical properties of the fluid ρ_k and h_k are averaged over the control volume, while the mass flow rate is evaluated at the interface. In order to have a more straightforward notation, for each control volume, the outlet mass flow rate is called $\dot{m}_{out,k}$. Moreover, the refrigerant enthalpy must be evaluated at the cell's boundary to close the energy balance for the refrigerant. According to [10], the value of the refrigerant enthalpy at the outlet is assumed equal to the lumped enthalpy for each cell, in order to reduce numerical instabilities connected with linear interpolation.

In this way, for each control volumes (k) the mass balance equation becomes:

$$V_k \left[\left. \frac{\partial \rho_k}{\partial P} \right|_{h_k} \frac{dP}{d\tau} + \left. \frac{\partial \rho_k}{\partial h_k} \right|_{P} \frac{dh_k}{d\tau} \right] - \dot{m}_{out,k-1} + \dot{m}_{out,k} = 0 \tag{5}$$

The energy balance for the refrigerant is rewritten as follows:

$$V_k \left[\left. \frac{\partial \rho_k}{\partial P} \right|_{h_k} - 1 \right] \frac{dP}{d\tau} + V_k \left[\left. \frac{\partial \rho_k}{\partial h_k} \right|_{P} + \rho_k \right] \frac{dh_k}{d\tau} - \dot{m}_{out,k-1} h_{k-1} + \dot{m}_{out,k} h_k = \dot{Q}_{r,k} \tag{6}$$

In case of $k = 1$ and $K = N$, the inlet or the outlet refrigerant mass flow rate and the inlet and the outlet refrigerant enthalpy respectively, are provided as inputs to the right hand side of the corresponding equations.

The final system of differential equation can be expressed in a compact form:

$$Z(x, u)x = f(x, u) \tag{7}$$

where the unknowns vector x is:

$$x = \left[\frac{dP}{d\tau} \left. \dot{m}_{out,k} \right|_{k=1:N-1} \left. \frac{dh_k}{d\tau} \right|_{k=1:N} \left. \frac{dT_{w,k}}{d\tau} \right|_{k=1:N} \right]^T \tag{8}$$

Only a subset of the unknowns vector x represents the time derivative of the state variables to be integrated with the chosen solver.

$$\dot{y} = \left[\frac{dP}{d\tau} \left. \frac{dh_k}{d\tau} \right|_{k=1:N} \left. \frac{dT_{w,k}}{d\tau} \right|_{k=1:N} \right]^T \tag{9}$$

Using this form it is possible to obtain the refrigerant mass flow rate at the boundary of each cell [8, 10]; which eventually leads to a more compact formulation, since the intermediate mass flow rates cancel out, [7, 9, 11].

2.1. Refrigerant heat transfer rate

The heat transfer rate $\dot{Q}_{r,k}$ for the working fluid in each zone is calculated through:

$$\dot{Q}_{r,k} = \alpha_{r,k} A_{r,K} (T_{w,k} - T_{r,k}) \tag{10}$$

where $\alpha_{r,k}$ is the heat transfer coefficient for the k^{th} element, and $A_{r,k}$ is the area of the heat transfer surface in the refrigerant side.

The physical properties of the working fluid averaged for each control volume are evaluated employing a suitable table compiled using the CoolProp library [13]. The heat transfer coefficient for the refrigerant side is calculated locally for each elements employing a set of two correlations depending on its phase:

- single phase in BP heat exchangers: Martin, [14],
- condensation: Longo et al., [15].

The heat transfer coefficients depend on the refrigerant mass flow rate in each element, which can be estimated with the linear interpolation of the mass flow rate at the boundary, [10]. In order to avoid numerical oscillations, the heat transfer coefficients are evaluated using an averaged mass flow rate defined as $\dot{m}_{avg} = 0.5(\dot{m}_{r,in} + \dot{m}_{r,out})$

2.2. Secondary fluid heat transfer rate

Since the two fluids involved in the process are counter-flowing, the heat transfer rate $\dot{Q}_{,k}$ of the secondary fluid in each control volume can be calculated with:

$$\dot{Q}_{s,k} = \dot{m}_s c_{p,s,k}(T_{s,in,k} - T_{w,k})(1 - e^{-NTU_{s,k}}) \tag{11}$$

where $\dot{m}_s$ is the mass flow rate of the secondary fluid, assumed constant along the BP condenser, $c_{p,s,k}$ is its specific thermal capacity at constant pressure, $T_{s,in,k}$ is the temperature of the fluid at the inlet of the control volume k^{th}, $T_{w,k}$ is the mean temperature of the wall, and $NTU_{s,k}$ is the number of transfer units:

$$NTU_{s,k} = \frac{\alpha_{s,k} A_{s,k}}{\dot{m}_s c_{p,s}} \tag{12}$$

where $A_{s,k}$ is the area of the exchange surface of the wall contained in the cell, and $\alpha_{s,k}$ is the heat transfer coefficient in the secondary fluid, calculated for each control volume.

The physical properties of the secondary fluid are evaluated at the inlet temperature for each cell $T_{s,in,k}$. The heat transfer coefficient is calculated with the correlation recommended by Martin, [14].

2.3. Model implementation

The FV model of a BP heat exchanger presented in this work is developed in the Simulink® environment, employing the *S-function* block, a powerful mechanism for extending the capabilities of this system by implementing code blocks written in Matlab® .

The boundary conditions for the system of equations constitute the inputs to be provided to the S-function block; these are the refrigerant mass flowrate at the inlet and outlet of the condenser, the refrigerant temperature at the inlet and the stationary mass flow rate and the inlet temperature of the secondary fluid.

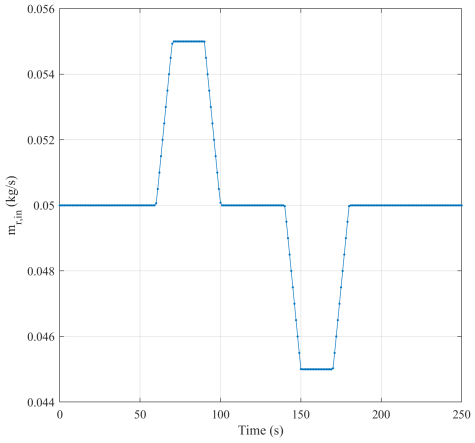

Figure 1: Inlet refrigerant mass flowrate.

Input	Value	Unit
$\dot{m}_{r,in,ref}$	0.05	kg/s
$\dot{m}_{r,out}$	0.05	kg/s
$\dot{m}_s$	0.28	kg/s
$T_{f,in}$	36	$°C$

Table 1: Fixed input values for the condenser SMB model during the test.

2.4. Analysis

The numerical test consists of a mass flow rate transient: all boundary conditions are kept constant, except the inlet mass flowrate of the refrigerant, which is subject to an increase of 10% of its initial value and then to an equal decrease before being brought back to its initial value. The input values used for the variables are summarized in table 1, while the temporal trend of the refrigerant mass flow rate at the condenser's inlet is shown in fig. 1.

The total heat transfer rate, the pressure of the working fluid, and the outlet temperatures of both fluids and the refrigerant mass inside the condenser have been chosen as monitored variables in order to evaluate the accuracy.

Numerical integration is carried out via four fixed step solvers available in Matlab®, *ode1*, *ode2*, *ode3* and *ode4*. In such a way is possible to study the effect of a higher-order solver on the accuracy of the predicted values of the variable. Assessing the dependence of the FV model on the fixed-step solver used can be very useful in order to employ it in control-oriented applications. Indeed, in a complex dynamical system, the integration step-size need to match the requirements at any given time of each of the integrated subsystems; so adopting a fixed step result in more robustness of the simulation. Moreover, a fixed integration step size can deal easily with sample input provided in real-time by appropriate acquisition systems [16].

According to previous work [9], the integration step size is explored from a $0.005\,s$ to $0.04\,s$, to evaluate its effect on the accuracy and stability of the model; attention is paid for correctly catching the simulation failures due to too big integration step. Finally the effect of the discretization is analysed, with the number of elements ranging from 5 to 100.

The normalized root mean squared error (NRMSE) is chosen as a metric for convergence. The NRMSE for each monitored variable (x) is calculated with eq. (13) using as reference signal (x_{ref}), corresponding to the calculated value using the ode4 solver with the minimum integration step-size ($0.005s$) and the maximum number of elements (100).

$$NRMSE = \frac{\sqrt{\frac{\sum\left(x_i - x_{ref,i}\right)^2}{N}}}{x_{max} - x_{min}} \tag{13}$$

3. Results ans discussion

In fig. 2 the time behaviour of three of monitored variable are plotted for the various combinations of solvers, integration step-size and elements number: pressure, total heat transfer rate and refrigerant outlet temperature. The reference simulation is highlighted with a thicker line: a clear convergence can be appreciated.

The effects of the solver's settings are evaluated using as a performance criterion the NRMSE averaged over all the monitored variable. Each plot in fig. 3 represents the NRMSE over the integration step size obtained employing a solver of different order; the levels of discretization are depicted with different markers; when the simulation fails the marker is absent. The same piece of information can be obtained from this plot. First, the accuracy of the model does not depend significantly on the integration-step size and on the solver order, indeed in all the plots each simulation with the same level of discretization leads to almost the same NRMSE independently of the step size. The number of elements of the grid has the most relevant effect: a good accuracy is reached with 25 elements; grids with more than 50 elements do not lead to a significant reduction in the NRMSE. Finally, it can be noticed that the simulation fails noticeably depending on the combined action of the step-size and discretization: indeed, the simulation does not converge when a large step-size is applied to a fine grid; in general, lower-order solvers are slightly more robust then higher-order ones in this situation. A grid with a maximum of 10 elements is stable for all the step-sizes tested ; when the number of elements increase the step-size needed shrinks; for grids with more than 50 elements, a step-size slower than $0.02\,s$ is required.

Figure 4 shows the comparison between the NRMSE and the real time factor (RTF), i.e. the ratio between length of time taken to run simulation and runs examined are characterized by a grid with more than 10 elements, because, from the previous analysis, a grid less refined yields an inadequate accuracy, and a RTF below than 0.5 must still be reached, to accommodate the demands of real-time systems. A good compromise between accuracy and computational time

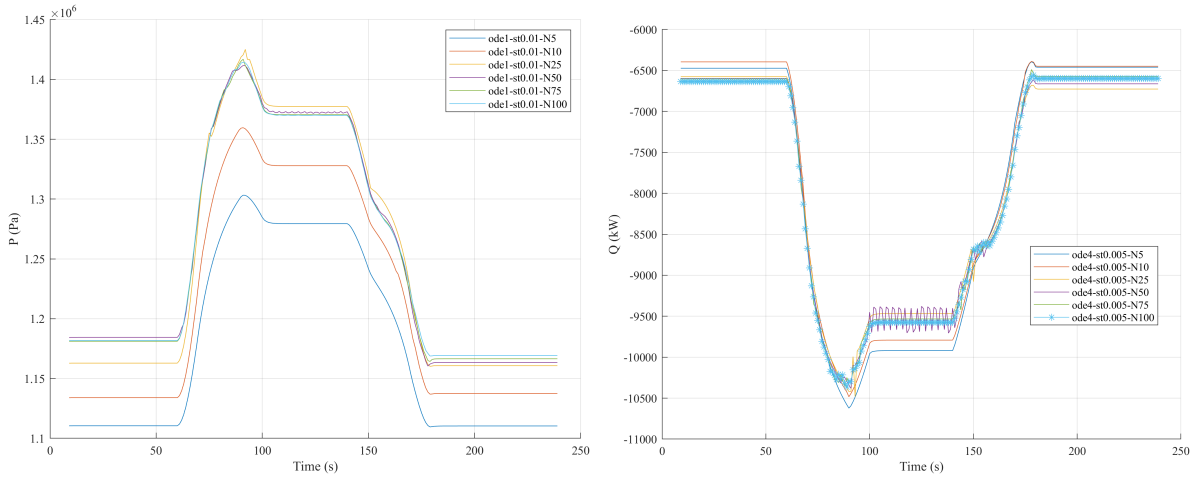

(a) (b)

Figure 2: Pressure (a) and heat transfer rate (b) time plots in the condenser for different combinations of solver, integration step-size and number of grid elements. In the legend, *ode* followed by a number indicates the Matlab® solver used, *st* the step size and *N* the number of elements.

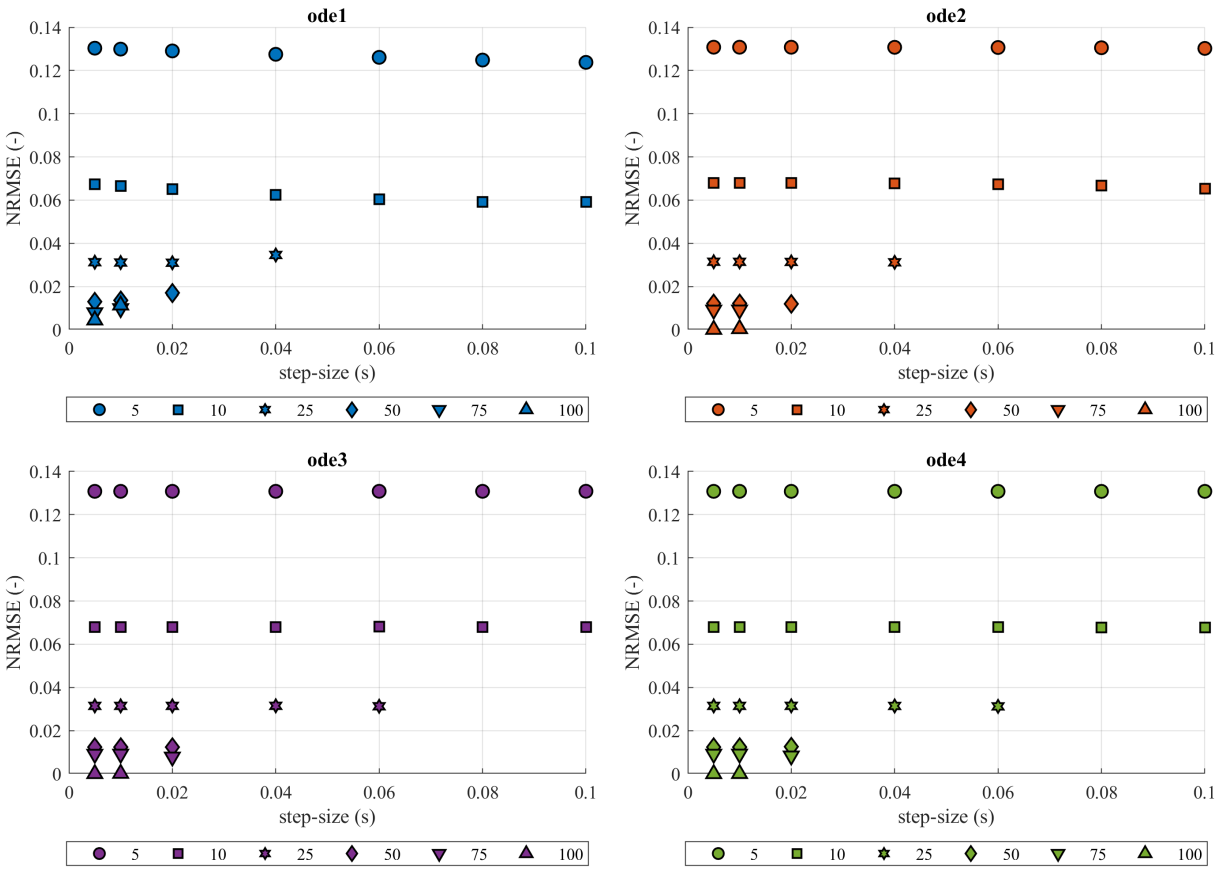

Figure 3: Numerical performance of the models.

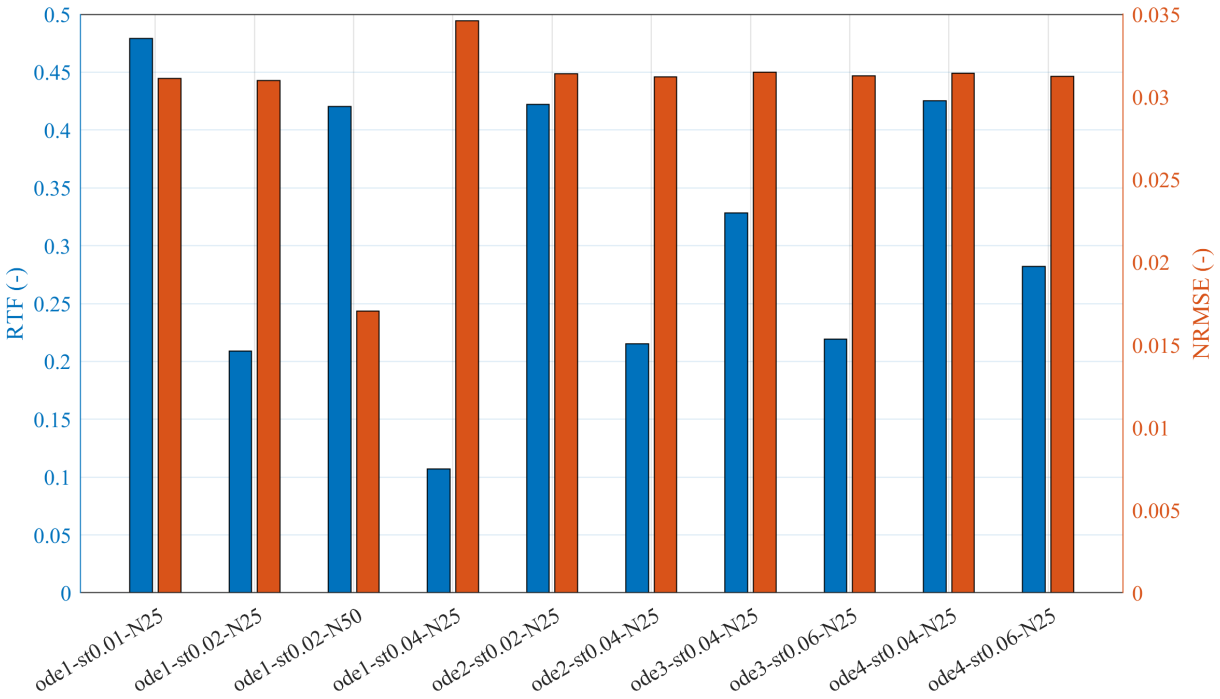

Figure 4: Comparison of the effect of solver selection, step size and number of elements on the real time factor and NRMSE. Only simulations with RTF lower than 0.5 are considered. In the axis labels, *ode* followed by a number indicates the Matlab® solver used, *st* the step size and *N* the number of elements.

is achieved by a solver of the second order with a grid of 25 to 50 elements.

4. Conclusions

In this work a finite-volume model of a brazed-plate condenser for vapour compression system applications was numerically verified, focusing on the effect of the solver order, of the integration step-size and of the mesh refinement on the accuracy of the predicted value of the monitored variables. Indeed, simulations using a fixed step are in general slower than those employing a variable step, yet the former approach is more suitable for integration in complex, control oriented real-time systems. It is shown that the discretization has the dominant effect on the accuracy of the model, in comparison to the integration step-size and the solver order. The number of elements should be chosen between 20 and 50 to guarantee both accuracy and stability. Finally, it is shown that a very good performance in terms of both RTF and accuracy is achieved with a solver of the second order.

5. Referecens

[1] Dupont, Domanski, Lebrun and Ziegler 2019 38th Note on Refrigeration Technologies: The Role of Refrigeration in the Global Economy (2019)
[2] Bendapudi S and Braun J E 2002 A review of literature on dynamic models of vapor compression equipment
[3] Rasmussen B P 2012 *HVAC&R Research* **18** 934–955
[4] Grald E W and MacArthur J W 1992 *International Journal of Heat and Fluid Flow* **13** 266–272
[5] McKinley T L and Alleyne A G 2008 *International Journal of refrigeration* **31** 1253–1264
[6] Li B and Alleyne A G 2010 *International Journal of refrigeration* **33** 538–552
[7] Rasmussen B P and Shenoy B 2012 *HVAC&R Research* **18** 956–973
[8] Salazar-Herran E, Martin-Escudero K, Portillo-Valdes L A, Flores-Abascal I and Romero-Anton N 2020-02-01 *International Journal of Refrigeration* **110** 83–94

[9] Bendapudi S, Braun J E and Groll E A 2005 *ASHRAE Transactions* **111** 132–148 ISSN 00012505
[10] Pangborn H, Alleyne A G and Wu N 2015-05-01 *International Journal of Refrigeration* **53** 101–114 ISSN 0140-7007
[11] Bendapudi S, Braun J E and Groll E A 2008 *International journal of refrigeration* **31** 1437–1452
[12] Rodriguez E and Rasmussen B 2017 *Applied Thermal Engineering* **112** 1326–1342
[13] Bell I H, Wronski J, Quoilin S and Lemort V 2014-02-12 *Industrial & Engineering Chemistry Research* **53** 2498–2508
[14] Martin H 1996-01-01 *Chemical Engineering and Processing: Process Intensification* **35** 301–310 ISSN 0255-2701
[15] Longo G A, Righetti G and Zilio C 2015 *International Journal of Heat and Mass Transfer* **82** 530–536
[16] Murray-Smith D J 2012 *Modelling and Simulation of Integrated Systems in Engineering: Issues of Methodology, Quality, Testing and Application* (Elsevier)